Towards a structural understanding of plant-microbiota interactions using cryo-EM techniques

Liedtke, J.

2

How advances in cryo-electron tomography have contributed to our current view of bacterial cell biology

Advancements in the field of cryo-electron tomography have greatly contributed to our current understanding of prokaryotic cell organization and revealed intracellular structures with remarkable architecture. In this review, we present some of the prominent advancements in cryo-electron tomography, illustrated by a subset of structural examples to demonstrate the power of the technique. More specifically, we focus on technical advances in automation of data collection and processing, sample thinning approaches, correlative cryo-light and electron microscopy, and sub-tomogram averaging methods. In turn, each of these advances enabled new insights into bacterial cell architecture, cell cycle progression, and the structure and function of molecular machines. Taken together, these significant advances within the cryo-electron tomography workflow have led to a greater understanding of prokaryotic biology. The advances made the technique available to a wider audience and more biological questions and provide the basis for continued advances in the near future.

This chapter is based on a published article by **Liedtke, J.**, Depelteau, J. S., and Briegel, A. (2022): *How advances in cryo-electron tomography have contributed to our current view of bacterial cell biology. Journal of Structural Biology: X*, 6, 100065.

2.1 Introduction

Microscopy has played a crucial role in gaining insights into the hidden world of bacteria. The ability to directly observe live bacterial cells has allowed us to gain insight into the basic biology of these organisms, such as their shape, growth and division cycles, and motility behaviours. With the advent of traditional electron microscopy (EM), the finer structural details of bacteria became clearer: differences in cell envelope structures could be distinguished, and the intercellular contents, such as the nucleoid and storage, could be identified. However, more detailed information could not be gained due to the nature of the sample preparation; Chemical fixation, dehydration, plastic embedding, and staining of the sample largely obscured the delicate ultrastructure of the bacterial cells (Figure 2.1 A). Subsequently, the usefulness of EM was thought to be limited and significant advances in genetic engineering and the development of fluorescent tags rendered EM a niche method. Therefore, despite increasingly detailed insights into the biology of bacterial cells gained by such alternative microbiological methods, many structural aspects of bacteria remained obscure. This lack of insight is still evident in the typical cell architecture comparisons between eukaryotic and bacterial cells in textbooks. While eukaryotic cell types were known to contain a myriad of structures, such as a diverse cytoskeleton, Golgi apparatus, and mitochondria, bacterial cells were often depicted with a generic rod-shaped cell containing only a nucleoid, ribosomes, cell envelope layers, and occasional appendages (Figure 2.1 B).

The introduction of cryogenic electron tomography (cryo-ET) made it possible to elucidate the finer structural features of bacterial cells in a near-native state, in three dimensions, and at macromolecular resolution. To do this, the bacterial cells are flash-frozen on an EM support grid in a liquid-nitrogen-cooled cryogen [17]. This freezing process is so fast that water molecules do not form ice crystals. Instead, the sample is embedded in a glass-like state (referred to as vitrification) that preserves the delicate ultrastructure of the cells [14, 17]. Vitrified samples are then imaged using a cryogenic transmission electron microscope (cryo-TEM). The cryo-TEM collects a series of 2-dimensional (2D) images while the sample is being tilted with respect to the electron beam. The resulting set of images, referred to as a tilt-series, can then be computationally back-projected to generate a 3-dimensional (3D) volume of the target (referred to as a tomogram). However, the potential impact of this workflow, called cryogenic electron tomography (cryo-ET), on the current understandings of bacterial ultrastructures was not immediately realized by microbiologists. A decade after its advent, the Baumeister group first applied this technology to prokaryotic cells in 1998 [18]. Even still, only a small number of studies used this method on bacterial cells for an additional decade [19].

Today, cryo-ET is widely recognized as a powerful tool to unravel the structural aspects of microbes. This method has greatly contributed to our understanding of how microbes are structurally organized, how they grow and divide using a highly complex cytoskeleton, and how they use molecular machines such as secretion systems, cell appendages, and chemotaxis arrays to navigate and interact with the environment (Figure 2.1 C). In its early days, data collection was practically manual, requiring constant supervision. However, automation of the technique quickly advanced and the data collection process is now largely self-operating. In addition, improvements in the hardware, such as new types of

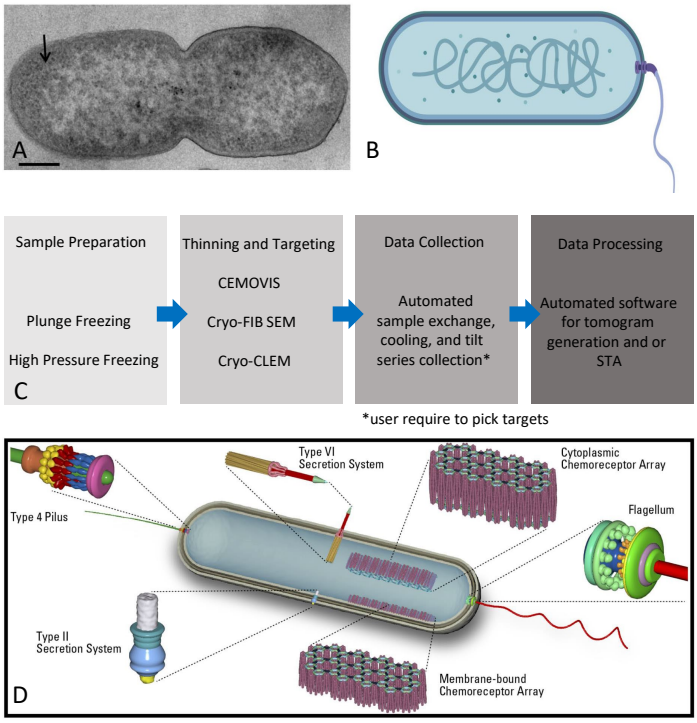

Figure 2.1: Changing view of the bacterial cell structure. (A) Traditional EM image of *Pseudomonas aeruginosa* (arrow indicates tightly packed material). Image reproduced from Latino *et al.* (2019) [20] with permission. (B) Simplified schematic of a bacterial cell, lacking structural detail (made in Biorender.com). (C) Workflow of cryo-electron tomography. (D) Modern interpretation of a bacterium, containing selected structural features (schematic by Robert van Sluis).

cameras/detectors, the ability to section cryo-preserved samples at cryogenic temperatures, the development of correlative techniques with fluorescent light microscopy, and new software packages to analyse the data, aided in raising cryo-ET to a key method in the prokaryotic biology toolbox. In this review, we will highlight some of the important insights gained by the improvements of cryo-ET. However, cryo-ET has so extensively contributed to our current understanding of the structure of bacterial cells that we will only highlight some selected structural examples.

2.2 Cryo-ET automation exemplified insight into bacterial cytoskeleton

Following its proof of concept, cryo-ET was first practically used to describe novel cell attachment structures [18, 21]. These studies relied on only a handful of tomograms since data collection and processing were time-consuming and mostly manual. Specifically, data collection had to be supervised to ensure proper imaging conditions throughout the tilt series, such as accurate target tracking and maintaining defocus settings of the individual

images. The subsequent processing of the 2D images to generate the tomograms was equally taxing. For instance, the early software programs, such as the EM software [22], required the user to manually track gold particles in each image. These gold beads are typically added to the sample before freezing to allow for an accurate alignment of the images of a tilt series, which is necessary for a precise 3D reconstruction.

This highly manual workflow resulted in a low throughput of data acquisition and processing, which in turn greatly limited insights into many aspects of bacterial cell biology. The development of robust cryo-ET data collection software provided the means for a higher sample throughput (for example TOM toolbox, UCSFtomo, FEI software, serialEM) [23–25]. In addition, technical improvements such as maintaining liquid nitrogen cooling of the samples enabled automation of tilt-series collection without supervision. Automation increased the number of tilt-series collected, which necessitated the creation of automated post-processing routines such as IMOD and Warp [26, 27]. These new softwares allowed for an automatic transfer of the images to the processing platform, and subsequent automatic processing using batch routines. A good description of the data processing steps can be found for example in the article of Baldwin *et al.* (2018) [28]. In addition to the technical developments directly related to instrumentation and software, advances in computational processing power with improved CPUs and GPUs, and the advent of direct electron detectors capable of collecting movies with high speed and improved accuracy, have aided in the increasing automation of the workflow as well as greatly improved image quality [28]. Together, these improvements not only result in more reliable data but also increase the amount of higher resolution information available for analysis. These advancements directly led to a better understanding of the components of a complex system such as the bacterial cytoskeleton.

In eukaryotes, it has been long known that the cytoskeleton is an intracellular network system of filaments and tubules which defines the form and structure of a cell and gives them coherence in its spatial-temporal operations [29]. In contrast, bacteria were thought to lack cytoskeletal elements and therefore were devoid of any internal order. Later, it was discovered that bacteria contain homologs of eukaryotic cytoskeletal filaments, but many questions regarding their detailed structure and function remained. Homologs of all three main protein classes of the eukaryotic cytoskeleton were discovered in bacteria, for example, FtsZ (tubulin-like), MreB (actin-like), and CreS (intermediate filament-like). Of these, the first described protein of the bacterial cytoskeleton was FtsZ. This protein was shown to be essential for cell division in most bacteria. Bi & Lutkenhaus (1991) [30] were the first to visualize the FtsZ filaments by immuno-electron microscopy (Figure 2.2 A). In this study, the FtsZ filament localization at the division site was revealed. With this information, the authors proposed an FtsZ assembly model that proposed a complete ring formation of FtsZ filaments. However, the question of if the FtsZ filaments formed such a continuous ring or not remained.

While cryo-ET is very powerful in resolving structures in intact cells, determining their identity remains a challenge. At present, there are no easily applicable tags comparable to the fluorescent markers used in light microscopy. Instead, the identity of a structure of interest can be indirectly determined by imaging a variety of mutant strains, where the protein of interest is altered in some way. This includes overexpression, deletion or

depletions, non-hydrolysable variants, or chemicals affecting the protein polymerization. Images collected of these samples are then compared to the wild-type strain to convincingly identify the target structure. This requires a large amount of data to be collected and therefore requires a large degree of automation in the workflow to be feasible. This approach was used in an early cryo-ET study that compared cryo-ET data of several different FtsZ mutants in *Caulobacter crescentus*. This research gained insight into the time of appearance of FtsZ filaments in the cell cycle, their position, orientation, as well as their number and length. The cryo-ET data revealed that FtsZ forms filaments that are relatively short (~100 nm) and overlapping in vivo. The insights led to the proposition of the 'iterative pinching model' [31].

While early studies proposed that FtsZ does not form a complete ring in *C. crescentus*, its presence in other bacteria remained disputed [32, 33]. The reason for this lies in the 'missing wedge' artefact of the cryo-ET process: during tilt series collection, the sample can only be tilted +/- 60, resulting in missing information obtained from greater tilt angles. In reality, it obscures features perpendicular to the electron beam, which is most obvious in the absence of discernable features on the top and bottom of a cell. As a consequence, the FtsZ ring could not be visualized as a complete ring [32].

Newer cryo-ET studies support the idea that a complete FtsZ ring is not needed to drive successful cell constriction and division in several species besides *C. crescentus* (Figure 2.2). Yao *et al.* (2017) [33] visualized various bacterial species in different division stages (pre-, early, mid, and post constriction stage). Additionally, they utilized an open access cryo-ET database [34] and categorized the imaged cells in the mentioned stages, ultimately identifying 159 dividing cells of 47 species. They confirmed that FtsZ filaments can indeed be found in different lengths and forms. Furthermore, they highlighted that the constriction process takes longer than the lifetime of the individual FtsZ filaments [33]. Despite all these insights, many questions remain on the cell division process, especially in the orchestration of the FtsZ ring formation and constriction in the context of the growing number of proteins that are known to be involved in this process, together called the "Divisome". Cryo-ET may also help answer these open questions in the future.

An additional cytoskeletal protein found in bacteria is the actin-like MreB, which is involved in the positioning of peptidoglycan (PG) during lateral cell-wall growth and division. For a long time, it was believed that MreB forms extended and static helical filaments. However, cryo-ET revealed that MreB forms only short filaments [35]. These conclusions were confirmed by two fluorescent light microscopy studies that visualized MreB filaments and their behaviour in vivo [36, 37]. They showed that short MreB filaments move in a helical pattern around the inner membrane in the cytoplasm, guiding the PG synthesis machinery. The question still remained: what was the composition of the extended filament? Cryo-ET later revealed that the extended helical structures are in fact artefacts of the yellow fluorescent protein (yfp) tag [38]. These research results highlight the importance of the visualization of samples by cryo-ET to gain insight into the bacterial cytoskeleton (for a detailed review see Pilhofer *et al.* (2013) [39]).

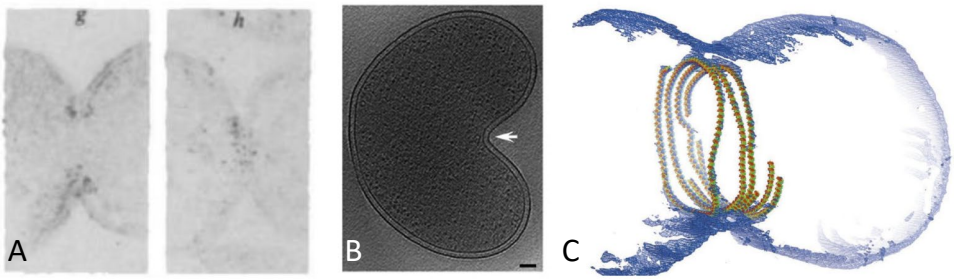

Figure 2.2: FtsZ structure; (A) comparison fro the first EM visualization of the FtsZ structure within *Escherichia coli* cell [30] with (B) the current models of symmetric constriction of a *Belliella baltica* cell (white arrow indicates the asymmetric division site) [33] and (C) a visualization of a semi atomic model of symmetric FtsZ ring constriction in a liposome [32].

2.3 CEMOVIS as a method to visualize cell envelope layers

A limitation of EM is the thickness of the prepared samples. When samples are too large, the entire electron dose is absorbed and all structural details are lost. Therefore, various techniques were developed to gain insight into the architecture of samples with a thickness beyond the scope of plunge freezing. Plunge freezing is an ultra-rapid cryofixation, whereby a thin layer of sample on a grid is so rapidly plunge into a liquid cryogen, that no ice crystal formation appears. Several thin-sectioning methods allowed the trimming of samples suitable for EM. Early methods are conducted at room temperature and involved harsh chemical treatments. In contrast to these classical sectioning types, cryogenic electron microscopy of vitreous sections (CEMOVIS) does not require chemical fixation or embedding in resin or plastic. Instead, samples are high pressure frozen, which vitrifies samples with high pressure and liquid nitrogen temperatures. As with plunge freezing, this sample preparation method preserves the delicate structure of the biological material. The frozen sample is subsequently transferred to a cryo-ultramicrotome and sectioned with a diamond knife into cryo-EM suitable sections [40].

The key difference between these techniques lies in the sample preparation, which is either chemical or physical nature. The chemical method is strongly dependent on the chemicals used for fixation, staining, and embedding, all of which can lead to serious artefacts. For example, one of the most famous artefacts is the mesosome which had been believed to be a compartment of the bacterial cell for years [41, 42]. However, with the application of the CEMOVIS technique, it was revealed that mesosomes are artefacts caused by chemical fixation [41, 42]. The obvious advantage of CEMOVIS is that it circumvents the artefacts associated with chemical treatment. The disadvantage of CEMOVIS is that it is not possible to combine it with immunogold labelling methods for structures inside of cells. However, it is predominantly suitable for structural investigation. Another disadvantage that both sectioning methods have in common are physical artefacts caused by the mechanical stress of sectioning, for example, knife marks and compression. Bleck *et al.* (2010) [41] compared the different sectioning methods with each other and concluded that even though CEMOVIS is not an artefact-free method, it is still the preferable method.

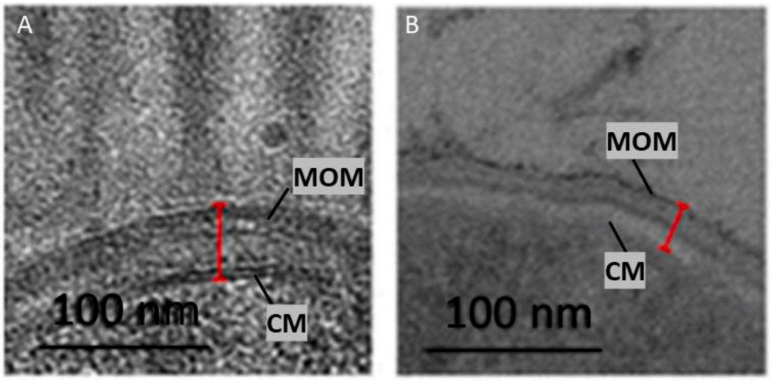

Figure 2.3: Comparative micrographs of *Mycobacteria smegmatis* cell envelope for the different sectioning types; CEMOVIS (A); and classical preparation with chemical fixation and resin embedding (B). Red line indicates the cell wall thickness, whereby the inner and outer membranes are easily detectable in A compared to B. Adapted from Bleck *et al.* (2010) [41]. CM, cytoplasmic membrane; MOM, mycobacterial outer membrane.

It provides a better understanding of biological structure within a cell and even tissue, which are usually too thick for direct imaging. For example, with CEMOVIS it was possible to image the cell envelope of mycobacteria and to confirm the existence of their unique cell envelope. The cell envelope is a multi-component, layered structure that is responsible for maintaining cell shape as well as protection from environmental stressors. Mycobacteria have an unusual outer membrane that consists mainly of mycoloic acid, a lipid that gets easily dissolved by chemical treatment. Thus, due to this characteristic, it was not possible to visualize it with the common sectioning methods and its existence was controversial until 2008 (Figure 2.3). CEMOVIS was crucial in confirming the presence of this structure.

2.4 Advances in sample thinning for cryo-ET

Since the introduction of cryo-ET, sample thickness has been a major limitation. The general rule within the community is that the maximum thickness of the sample is twice the power of the electron beam. Theoretically, this has been predicted to be slightly less, but other factors such as the contents of the sample can also play a role [43]. Thus, if you are working with a 300 keV instrument, the electrons will pass through a sample of up to 600 nm in thickness. However, it is important to consider that the increasing thickness of the sample also diminishes the availability of high-resolution information, thus limiting the questions that can be addressed.

About fifteen years ago, a technique typically used in material sciences called focused ion beam scanning electron microscopy (FIB SEM) was adapted to work at cryogenic temperatures and was shown to be suitable for vitrified biological samples [44]. Now referred to as cryo-FIB SEM, the technique preserves the vitreous nature of the sample while using the focused ion beam to systematically remove material from the sample until it is sufficiently thin. The SEM beam is used during this process to monitor the progress of the thinning process. Cryo- FIB SEM has evolved into a valuable method to thin plunge

frozen samples that are otherwise too thick for cryo-ET, and has been used to study a variety of samples and biological questions [45, 46].

The power of this technique was recently demonstrated by the identification of the structural proteins associated with endospore formation. These spores are highly resistant to environmental stresses and can endure for extended periods due to a thick, protective protein coat. For some bacterial species, like *Bacillus subtilis*, this dense coat prohibited direct visualization by cryo-ET. However, Khanna *et al.* (2021) [47] were determined to understand the sporulation processes of *B. subtilis*. Previous research had shown that the process of sporulation was significantly different from the division during vegetative growth, though exactly how was unknown [48, 49]. To solve this problem, Khanna *et al.* (2021) [47] used cryo-FIB SEM to first thin the cells to approximately 200 nm, which were then subsequently imaged (Figure 2.4 A) [47]. Remarkably, they were able to show that the FtsZA division machinery is evenly distributed along the division septum in vegetative cells (Figure 2.4 B). Conversely, in sporulating cell, the FtsZA is not distributed evenly along the septum but rather located only on the mother cell side of the septum (Figure 2.4 C). Using a combination of genetic and imaging techniques, they had further shown that this asymmetry is likely due to SpoIIE localization on the spore side of the septa, which lead to an exclusion of FtsZA and resulted in a thinner division septum. Cryo-FIB SEM, followed by cryo-ET, was essential to gain this important structural insight into spore formation.

Additional advancements in cryo-FIB SEM are currently in development. For instance, most studies using this technique have involved samples that can be prepared by plunge freezing to generate tiny sample fraction, called lamella. 200 nm lamella are easily produced in samples that are less than 5-10 µm in starting thickness. The next revolution in cryo-FIB SEM will be the processing of large-volume samples that require high-pressure freezing, which currently includes thicknesses of around 250 µm. This type of sample includes small multicellular organisms such as *Caenorhabditis elegans* and bacterial biofilms [45, 50]. Two primary methods in development are the 'lift-out' technique using a mechanical arm called micrograpper and focused ion beam milling with oxygen plasma [51–53]. Combined with the ion beam, the lift-out device allows for the excision of chunks of tissue from a large volume sample. These thinner samples are then transferred to a specialized grid for further thinning to create lamella for imaging. The oxygen plasma beam has been demonstrated to ablate larger volumes of HPF tissue without damage to the tissue and in less time, thus providing an alternative to the cryo-lift-out and current Ga+ FIB beam. These techniques have already been used in large volume samples such as *C. elegans*, however they are not yet readily available to the scientific community [52].

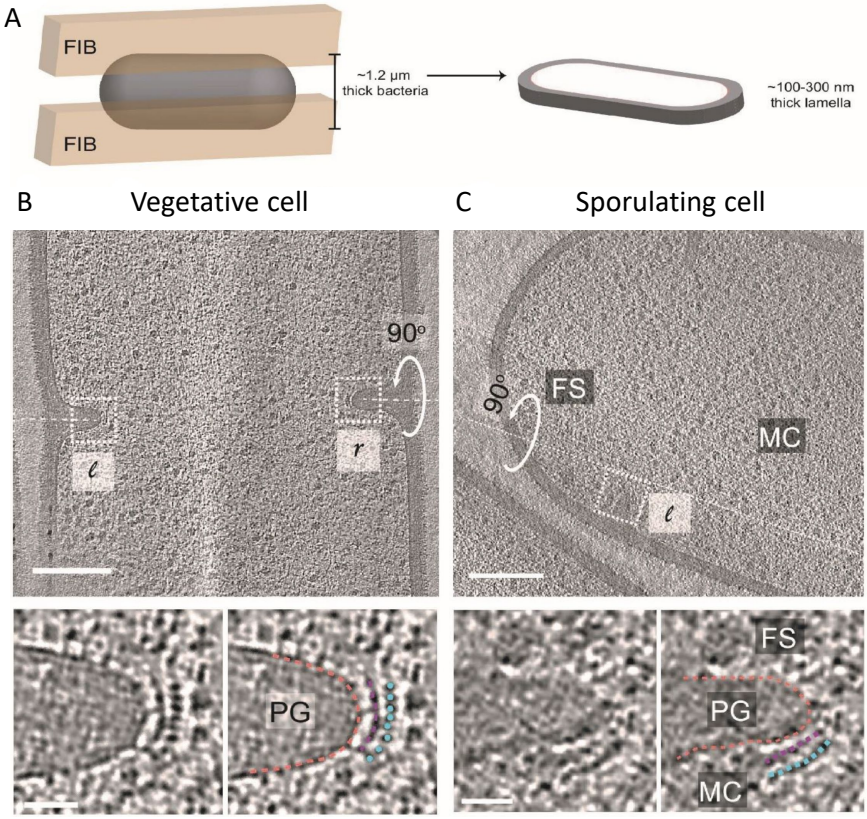

Figure 2.4: Schematic representation of cryo-FIB milling of the bacterial cell (A). (B & C) By thinning of *Bacillus subtilis* using cryo-FIB SEM, Khanna *et al.* [47] were able to identify the location of FtsZ (blue) and FtsA (purple) at the division septum for vegetative (B) and sporulating cells. Adapted from Khanna *et al.* [47].

2.5 Cryo-CLEM is a method that provides the distinction of compartments of a structure

The absence of widely applicable labels for cryo-ET to confidently identify a feature of interest in a tomogram remains a challenge. However, combining cryo-ET with fluorescence light microscopy (FLM) at both room and cryogenic temperatures (referred to as correlated light and electron microscopy, CLEM) can help to alleviate this issue. This combination allows structures of interest to be tagged with a fluorescent probe, imaged using a light microscope, and then prepared for and imaged with cryo-EM. At room temperature, challenges include the need for the sample to remain static during FLM and cryo-fixation; otherwise, the two images cannot be properly correlated. In addition, the resolution limitation of FLM often makes it very difficult to accurately identify the structure of interest. Despite these challenges, this method has been successfully used to determine the location of the chemotaxis arrays, the CTP synthase filaments, and the diffusion barriers in the bacterium *Caulobacter cresecentus* [54–56].

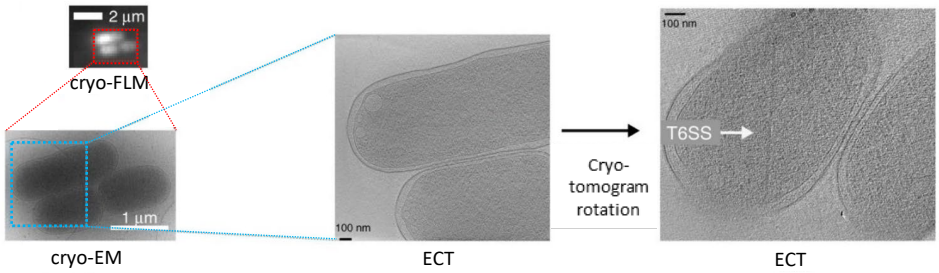

Figure 2.5: Cryo-FLM workflow used in the identification of the extended T6SS in enteroaggregative *E. coli*. The cells were first vitrified and then imaged by cryo-FLM to identify the cells that contained the Hcp1-CouAA labeled T6SS. Subsequent cryo-ET and rotation of the tomogram in the area of interest led to the visualization of the T6SS. Adapted from Szwedziak and Pilhofer (2019) [58].

With the introduction of cryogenic CLEM (cryo-CLEM), the sample is first frozen, immobilizing the structures in place, and then imaged using the typical cryo-FLM and cryo-EM workflow. This technique has been used to identify and describe several prokaryotic structures, including the MreB filaments in *C. crescentus*, and the type 6 secretion system (T6SS) [35]. First observed in Vibrio cholerae, the T6SS is a syringe-like structure found in some gram-negative bacteria [57]. The T6SS acts as a molecular needle that contains effector molecules used to stave off offending bacteria or to occupy new environmental niches. It consists of a membrane-bound inner tube and spike structure surrounded by a sheath assembly that is responsible for the contraction and injection. Bound to the membrane at the proximal end, the process of contraction results in a rearrangement of the sheath proteins causing the effectors located inside the tube to be shot into the neighbouring cell. Disassembly quickly follows, allowing the sheath subunits to be re-used in the formation of a new T6SS.

A recent example of the use of cryo-CLEM in the study of T6SS was shown by Szwedziak and Pilhofer (2019) [58]. In this study, the authors examined T6SS in enteroaggregative *Escherichia coli*, identifying a subset of T6SS structures that were connected to the membrane at both the proximal and distal ends of the sheath/tube complex (Figure 2.5). Cryo-CLEM was integral in the identification of the T6SS in this model, providing adequate data to then model the behaviour of contraction at both ends of the needle.

Advances in the cryo-FLM portion of the workflow will allow for better correlation of the fluorescent signal with the cryo-ET data. For example, the development of cryogenic photoactivated localization microscopy (cryo-PALM) combined with cryo-ET allowed the identification of the T6SS in the bacterium, *Myxococcus xanthus* [59]. Without the cryo-PALM, the T6SS is challenging to distinguish from other tubular structures present in this bacterium. By tagging the sheath protein VipA with a photoactivatable GFP, the authors were able to locate the structure within the cell in multiple states and with increased precision. This is just one example of the potential power that CLEM can have in identifying and understanding the various molecular machines in prokaryotes.

2.6 Subtomogram averaging to gain insight into molecular machines: Chemotaxis and Flagellar Motors

As illustrated above, cryo-ET has proven to be a powerful technique. However, the tomograms are typically not sufficient to determine the structure and function of molecular machines in situ. This is due in part because the signal-to-noise ratio, a ratio between the desired signal and the background, is too low to determine the detailed composition of macromolecular complexes. If the background noise is equal to or higher than the signal noise then the target structure cannot be differentiated from the background [60]. This is the case for typical cryo-ET datasets because the data is acquired using low dose schemes to lessen the electron damage to the sample. This limitation can be partially overcome for certain cellular content that has a consistent, identical structure. In this case, we can apply a method where the identical structures are computationally extracted in so-called sub-volumes. These are then aligned to match in orientation and averaged. The resulting EM map of such an average has a substantially increased signal-to-noise ratio that allows the interpretation of structural details at higher resolution. This technique is referred to as sub-tomogram averaging (STA) [60]. STA also helps to minimize the effect of the missing wedge artefact if the particles within the individual sub-volumes have different orientations. Thus, with more particles, this artefact becomes less severe. Several dedicated specialized software packages allow STA, such for example PEET, TOM toolbox, Dynamo, EM clarity, M-software, EMAN, or Relion [28, 61]. While these all have their specific advantages, they all can extract, align and average sub-volumes that have been extracted from 3D volumes. The packages also conduct missing wedge orientation and compensation by replacing particles with information from other particles containing this specific region [28]. This additional data processing of cryo-ET data has provided some breakthrough insights into the structure and function of two macromolecular machines that enable the cells to sense their environment and actively move toward beneficial environments: the chemoreceptor arrays and flagellar motors.

Chemotaxis is a behaviour that allows the bacteria to sense their chemical surroundings and control their motility apparatus to seek out their preferred environmental niches and evade harmful ones. The bacterial chemotaxis system in the bacterium *E. coli* is arguably the best-studied signal-transduction system in biology. It relies on chemoreceptors called methyl-accepting chemotaxis proteins (MCPs), a histidine kinase CheA and the coupling protein CheW. These functional units cluster together to form extended arrays at the cell poles, which can contain thousands of chemoreceptors. In the presence of repellents or absence of attractants, CheA triggers the response messenger CheY by phosphorylation. CheY-P in turn binds to the flagellar motor and modifies the direction of flagella rotation. Additional proteins (CheR and CheB) modulate the response, enabling the cells to follow chemical gradients. CheZ terminates the cycle by turning off the respond messenger protein CheY. Chemoreceptor arrays are highly cooperative, and the activation of one receptor can spread through the array.

While the individual components of this system have been well-studied in the past, the structure and function of the in vivo arrays were unknown until they were imaged

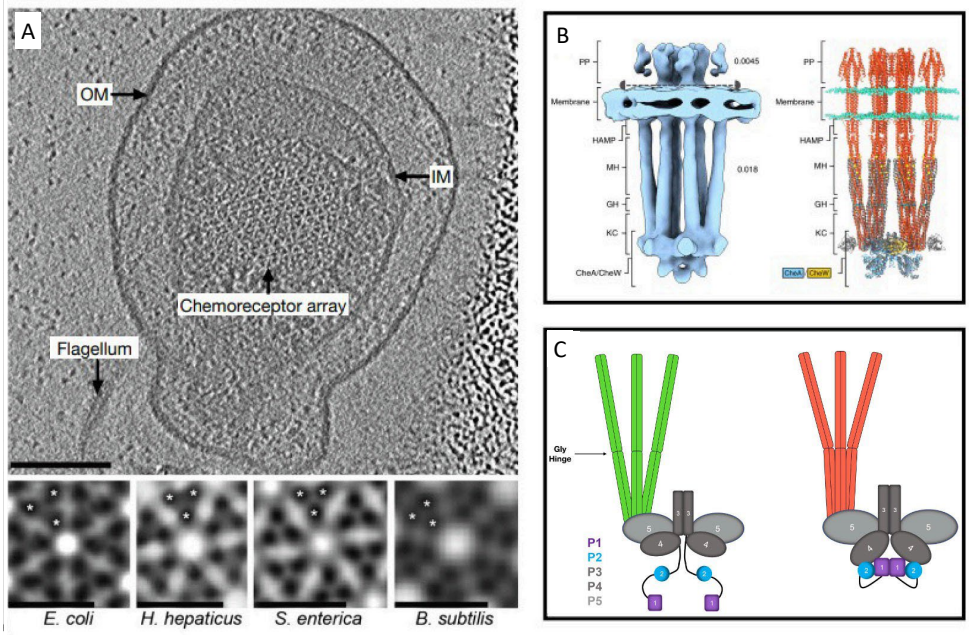

Figure 2.6: (A) Top: Top view of a chemotaxis array in a *Salmonella enterica* minicell. IM: inner membrane, OM: outer membrane. (A) Bottom: Subtomogram averages of chemoreceptor arrays in diverse species, highlighting the universal receptor arrangement. Reproduced with permission from Briegel *et al.* (2012) [62]. (B) Left: STA of the functional unit. PP: periplasmic ligand-binding domains, MH: methylation-helix bundles, GH: flexible regions containing the glycine hinge, KC: kinase control region. Right: Molecular model. Red: receptors, blue: CheA, gold: CheW. Reproduced with permission from Burt *et al.* (2020) [64]. (C) Schematic representation of the structural changes between the kinase-off (left) and kinase-on states (right). Courtesy of Dr. Alise Muok [65].

by cryo-ET. Insights into the more detailed architecture of the arrays and the changes following activation could only be gained using STA. STA revealed the architecture of these arrays, where the hexagonal receptor arrays are networked by rings of alternating CheA and CheW monomers [62, 63].

In addition, STA of in situ arrays in combination with molecular dynamics flexible fitting (MDFF) revealed insights into the structural changes that occur during the activation of CheA. The receptor-trimers adopt a more closed conformation at their baseplate interacting tips in the inactivating state, and a more open, splayed conformation in the activating state [66]. STA further revealed changes in the structure of the kinase between the on- and off states. In the off state, the two CheA domains that contain the phosphoryl group for transfer to the response messenger, as well as the domain responsible for the docking of the CheY protein, are bound to the rest of the protein in an unproductive manner (Figure 2.6 C). Once activated, these two domains are released, allowing for CheY binding and phosphoryl transfer [67]. With ever-increasing resolution of STA, it can be expected that soon further details of the signal-transduction will be unrevealed. This will undoubtedly help to understand still open questions on how the different components of the chemotaxis system interact with each other and how they are controlled.

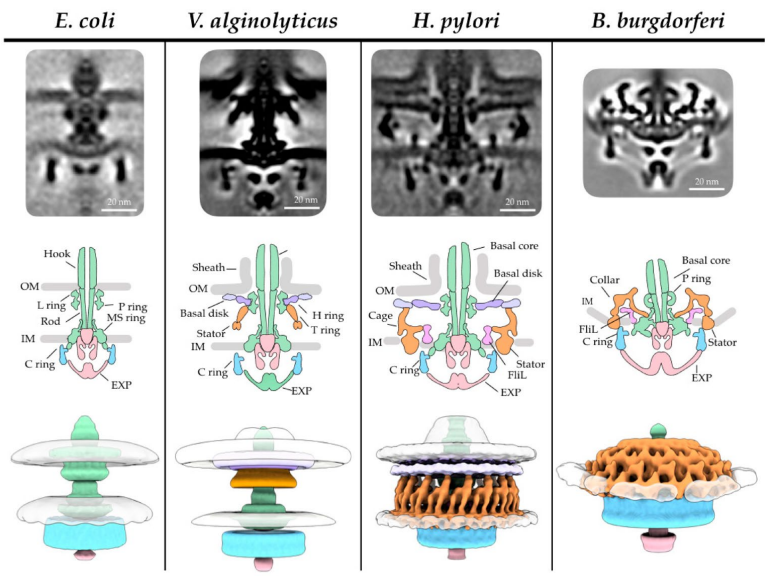

Figure 2.7: Flagellar motor, showing the conserved core elements as well as the species and genera-specific motor adaptations to fulfil their needs in their specific environment. Adapted from Carrol and Liu (2020) [68].

Another well-understood macromolecular complex is the flagella motor which powers flagellar rotation. Flagella are extracellular appendages that provide the cells with the ability to move, either by swimming through a liquid medium or by swarming on surfaces. The flagellum consists of a basal body (motor), a hook (flexible linker), and a propeller (helical filament). It is attached to the flagellar motor, which extends from the cytoplasm, through the inner membrane and the peptidoglycan layer (periplasmic space), to the outer membrane. In general, the core of the flagellar motor is structurally well conserved and shares the same mechanism among species, but the entire motor structure varies greatly (Figure 2.7). Depending on the species, the motor is either powered by a proton-motive force or by ion-motive force. In *E. coli*, depending on the orientation of the filament rotation the cell either swims/runs (counter-clockwise rotation, CCW) or tumbles (clockwise rotation, CW). The motor rotation is biased by the binding of the phosphorylated CheY from the chemotaxis system. A more detailed description of the flagellum and the flagellar motor composition can be found in the review of [68].

In the past years, STA was not just used to reveal species-specific flagellar motor compartments. It also investigated how the components interact with each other. A recently revealed example is the interaction between the messenger protein CheY with the C-ring (FliM, FliN, FliG). CheY binds to FliM and leads to a major conformational change of FliG, while FliN prevents disassociation of the C-ring compounds during the conformational change. In turn, the conformational change of FliG leads to a remodelling of the rotor-stator interaction and a switch from a CCW to a CW tumble rotation of the filament [69]. The rotor and stator complex are known to be highly dynamic and the moment of switching is rather volatile, and therefore difficult to visualize. A described solution to

improve the visualization is to increase the density of the small switching proteins by GFP labelling and/or using homologs with a higher molecular mass in combination with STA [70]. In general, with increasing resolution, cryo-ET and STA will likely aid in revealing other aspects of the flagellar motor soon. For example, binding affinity vs. competition, stator assembly, and relative orientation of c-ring components are still not fully understood yet and might be answered in the coming future.

2.7 The future of cryo-ET

As we, and many others, have described, cryo-ET has evolved tremendously over the past twenty years, due in part to the work of Baumeister and his scientific heritage. Advancements in the field will continue in the years to come, significantly enhancing our knowledge of prokaryotic cell biology. Those enhancements include improved sample preparation workflows, advances in hardware and software, and the curation of the vast amount of data into publicly available resources.

Sample preparation is one of the key steps in the cryo-ET workflow. Without a properly prepared sample, no subsequent step is likely to succeed. In the past few years, significant developments in plunge freezing technologies allow the combination of grid preparation, sample application, and freezing into a single device [71, 72]. In addition, the advent of inkjet-like printing technologies and the introduction of self-blotting grids will enable the study of very volume-limited samples, which was previously impossible [73]. As noted in the large volume section, thicker samples are also becoming more and more accessible. With the application of the cryo-FIB SEM, plunge frozen samples can currently be thinned. The development of tools for larger volume samples such as multicellular tissues will greatly increase our understanding of how microbes interact with their environment.

Hardware and software developments will continue to increase the amount of data collected as well as our ability to process this data for valuable information. Hardware developments such as the laser phase plate, which provides increased contrast will minimal defocus, will likely allow a typically challenging technique to be applied to a wider range of samples with increased consistency [74]. Most importantly, the addition of this tool will aid in the analysis of smaller complexes and better interpretation of tomograms to a higher resolution. Software developments include those that enable fast tomography, a collection method that continuously records a movie as the sample is tilted with the electron beam on the sample [28, 75, 76]. Instead of the repetitive process of tilting, tracking, and imaging, these steps are essentially combined to produce one movie per target. Depending on the collection scheme, fast tomography could increase collection time per target by 50-75%, vastly multiplying the amount of data that can be collected per sample. The introduction of new processing programs such as Warp and M provides important information during data collection and a processing pipeline that connects the data collection directly to the tomogram and ultimately structural analysis [27, 77]. Software improvements are also impacting the sample preparation steps. For instance, for cryo-FIB SEM processed samples, the development of scripts has now begun to automate a typically slow and tedious process, which will lead to increased output and improved consistency [78, 79].

Once the data is collected, accessibility by the scientific community becomes important. Research groups typically focus on a single part of the data or are looking to answer specific

biological questions. Yet, cellular cryo-ET collects an abundance of information about the cell and much of this information is ripe for examination. Resources such as the Caltech Electron Tomography Database have laid the groundwork for building comprehensive collections of cryo-ET data, at least at the single group level [34]. In turn, some of this information has been translated into the Atlas of Bacterial and Archaeal Cell Structure [80]. This open access, digital resource provides detailed information about the prokaryotic ultrastructure of 85 species, which can be used as a source for comparison of structures in different strains, education, and comparison of sample treatments. Initiatives like this are extremely valuable to the community and should be a goal of the cryo-EM community.

Together, this review highlights the impact and advancements of cryo-ET since its application in 1998. The technique has proved to be a valuable tool that is only now reaching its potential. We look forward to the future where cryo-ET is a standard part of the microbiology toolbox.

Credit authorship contribution statement

Janine Liedtke: Conceptualization, Writing – original draft, Writing – review & editing. Jamie S. Depelteau: Conceptualization, Writing – original draft, Writing – review & editing. Ariane Briegel: Conceptualization, Writing – original draft, Writing – review & editing, Supervision.

Declaration of Competing Interest

The author declare that they have no known competing financial interest or personal relationship that could have appeared to influence the work reported in this paper. This work was supported by the OCENW.GROOT.2019.063 and Building Blocks of Life Grant 737.016.004 grants from the Netherlands Organization for Scientific Research (NWO).